New Framework for Deploying Grid Forming Services via Triggering Mechanism in the System Support Services Market

Louis Goonasekara, Lasantha Meegahapola, Shuo Yan
School of Engineering, RMIT University, Melbourne, Australia

***Abstract*—The accelerating transition to renewable energy involves the decommissioning of synchronous generators (SGs) and their replacement with inverter based resources (IBRs). This shift has created critical reliability challenges, manifesting as low system inertia, reduced short circuit ratio (SCR), and high rates of change of frequency (RoCoF) during disturbances. While grid forming inverters (GFMIs) are the ideal SG replacement, emulating the necessary virtual inertia and voltage source characteristics, most existing grid supporting services rely on traditional, less capable grid following inverters (GFLIs). This paper proposes a novel GFMI triggering framework that utilizes online inertia and real time SCR measurements. The mechanism prioritizes immediate active or reactive power support by evaluating detected shortfalls against their predefined critical boundaries (critical inertia and critical SCR). The framework is tested on the renewable integrated New England 39 bus system under two distinct contingency scenarios. The comparative results indicated a significantly faster response and improved system support services provided by the proposed framework compared to conventional deadband operated GFMIs, validating its effectiveness in stabilizing weak grid conditions. Furthermore, these findings emphasize the critical need for necessary tertiary control layer innovation towards separate and dedicated GFMI services.**

***Index Terms*—Ancillary services, grid forming inverter, online inertia, short circuit ratio, system support services, virtual synchronous generator, weak grid.**

I. Introduction

The reduction of synchronous generators due to the integration of Inverter Based Resources (IBRs) has caused the depletion of key essential characteristics from the power grid. Low inertia and low system strength are the key attributes of a weak power system that is prone to instabilities under minor contingencies. Synchronous Generators (SGs) are inherently capable of supporting voltage fluctuations effectively via its reactive power capabilities and arrest rapid frequency excursions using its stored kinetic energy as an inertial response. However, IBRs, do not have such high short circuit capacity and inertial response capabilities that could assist in fault conditions unlike SGs. Therefore, Grid Forming Inverters (GFMIs) have become highly relevant in recent years due to these issues faced by conventional Grid Following Inverters (GFLIs) [1]. GFMIs have the ability to recreate SG properties using Virtual Synchronous Generator (VSG) type strategy for active power control. This give GFMIs a clear distinct advantage over GFLIs which act as constant current sources, in contrast where GFMIs operate as a voltage source.

The most prominent control strategy that enable GFMIs to provide virtual inertia is VSG control based active power control [2]. VSG can be viewed as a specific instance of droop control where inertia and damping is present which gives the advantage closely replicating SG characteristics [3]. Synthetic inertia emulation has become an imperative requirement in modern power grids as Rate of Change of Frequency (RoCoF) recovery ability has become weak due to the loss of active SGs in the power system. While GFMIs are seen as a optimal replacements for SG in a IBR sense, proper framework and guidelines have still not been established for GFMI core requirements or GFMI services by Transmission Network Service Providers (TNSPs). This paper aims to investigate the integration of online inertia and Short Circuit Ratio (SCR) at Point of Common Coupling (PCC) as a triggering factor for effective active and reactive power control. A key requirement for inertial support is the quantification of overall inertia in a system as well as the virtual inertia provided by IBRs. A few online inertia measurement techniques have been proposed based on numerical calculation real time and Phasor Measurement Unit (PMU) values based computation of inertia [4]–[7]. In terms of system strength quantification, SCR is regarded as the measurement index by TNSPs globally and different interpretations of SCR has been introduced to account for different grid dynamics. Most recent index being Site Dependent SCR (SDSCR) which accounts for inverter interaction. Grid Strength Impedance Matrix (GSIM) is an index that focuses on the admittance matrix and Impedance Margin Ratio (IMR) proposes a system strength analysis framework in frequency domain [8]–[10].

The rationality behind proposing a novel triggering mechanism for a dedicated grid forming service market is to improve the efficiency of GFMI performance compared to conventional deadband operated system and to facilitate the system service provision based on inertia and system strength violations. Globally, ancillary services such as Frequency Control Ancillary Services (FCAS) in Australia and Fast Frequency Response (FFR) in Ireland are procured through competitive bidding mechanisms [11], [12]. These fast acting services are typically provided by IBRs utilizing deadband based activation schemes. Such schemes are configured to trigger only when specific thresholds such as the Normal Operating Frequency Band (NOFB) are breached. Consequently, this reactive approach introduces an inherent latency, potentially increase the RoCoF and deepen the frequency nadir. In contrast, the proposed framework utilizes online inertia and SCR as primary triggering parameters. Since

979-8-3315-8138-1

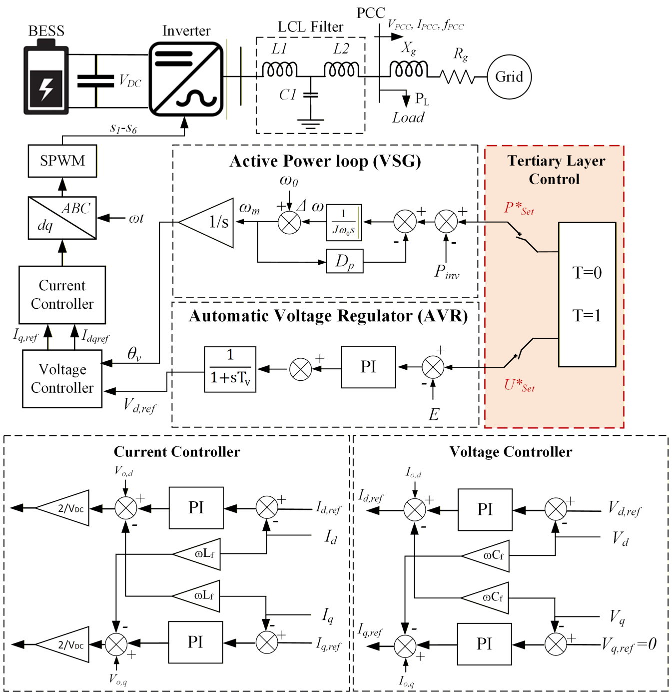

Fig. 1. Control architecture of VSG based GFMI.

shortfalls in these metrics can be identified pre-disturbance via generation schedules and load forecasts, this approach allows GFMI services to be positioned in a standby state, ensuring an immediate and robust response.

This study aims to investigate a tertiary layer control framework that can deliver GFMI services effectively via prioritizing either inertia-SCR or both via regulating active and reactive power. Section II of the paper introduces the proposed framework and Section III discuss the test system and weak grid performance of the entire controller.

II. Proposed Framework for Inertia and SCR Triggering based Active / Reactive Power Control

This section introduces the proposed framework for grid forming services using active and reactive power control via setpoint adjustment based on a triggering mechanism. The framework consists of two main components; the online inertia and SCR measurement framework and the triggering mechanism.

A. Online inertia measurement framework

The online inertia framework is established based on the kinetic energy principle indicated by (1) and (2) accounting for the synchronous inertia in the system.

$$E_{kinetic} = \frac{1}{2}\left[\sum_{n=1}^{k} J_k \omega_k^2\right] \tag{1}$$

$$E_{kinetic} = \frac{1}{2}J_1\omega_1^2 + \frac{1}{2}J_2\omega_2^2 + \cdots + \frac{1}{2}J_k\omega_k^2 \tag{2}$$

$E_{kinetic}$ is the kinetic energy, J_k is the moment of inertia (kgm^2) of the k^{th} generator, and ω_k is the rotor angular velocity in rad/s of the k^{th} generator. $E_{kinetic}$ is expressed in MWs units. The critical inertia computation is done based on an iterative technique using a frequency nadir approach. The swing equation (3) can be used to express the RoCoF as a function of $E_{kinetic}$ and $P_m - P_e$ shown in (4).

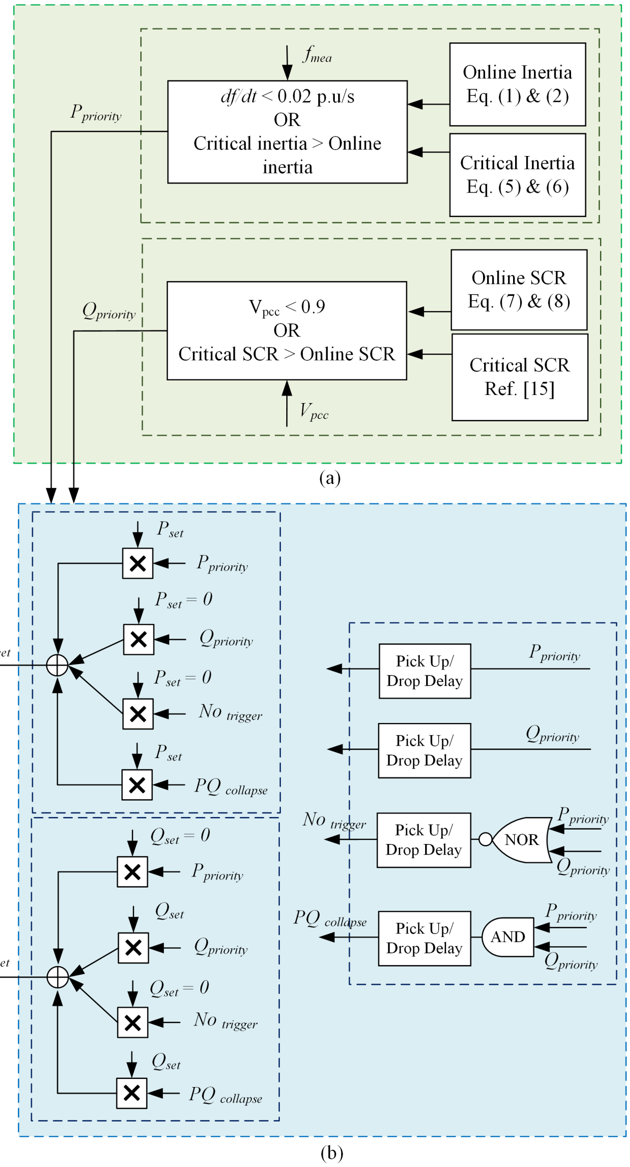

Fig. 2. Proposed GFMI tertiary control layer architecture, (a) online inertia and SCR triggering framework, (b) dynamic active / reactive power setpoint controller.

$$2H_k\frac{df}{dt} = P_{m,k} - P_{e,k} \tag{3}$$

H_k being the inertia constant of the k^{th} generator, df/dt being the RoCoF, $P_{m,k}$ is the mechanical power and $P_{e,k}$ is the electrical power of the generator.

$$\frac{df}{dt} = \frac{f_o}{2E_{kinetic}}(P_{m,k} - P_{e,k}) \tag{4}$$

f_o is the nominal frequency and $(P_{m,k} - P_{e,k})$ is active power deficit seen by the SG. Hence, this can be expressed as ΔP, the disturbance size. Throughout this study for critical inertia

979-8-3315-8138-1

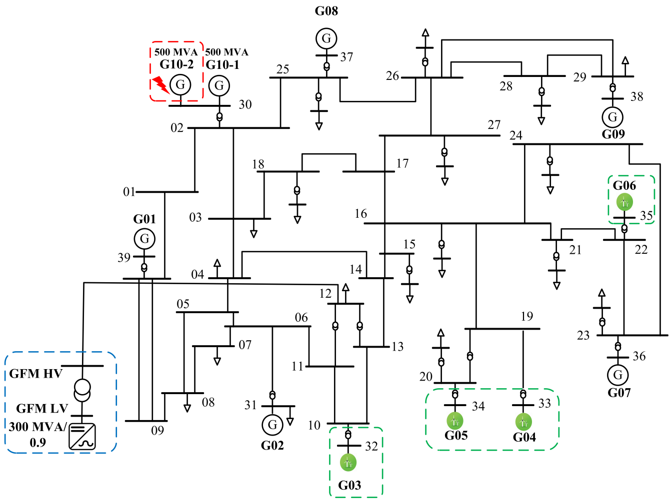

Fig. 3. Renewable integrated NE 39 bus system.

calculations ΔP will be assumed to be the loss of largest infeed into the power system.

$$E_{kinetic} = \frac{f_o}{2(\frac{df}{dt})}(\Delta P) \tag{5}$$

Lastly, the frequency nadir can be estimated using (5) and [13], [14],

$$f_{nadir} = f_o - \frac{f_o.(\Delta P)^2}{4Y_{sys}E_{kinetic}} \tag{6}$$

Y_{sys} is the aggregated ramp rate in MW/s units of all SGs in the system. The critical inertia calculation process is developed based on an iterative approach of calculating $E_{kinetic}$ using (5) until f_{nadir} in (6) reaches a pre-defined target frequency. The iterative calculation must meet two conditions.

- Following the loss of the largest infeed, initial RoCoF must remain below a threshold value defined by TNSPs.
- After the loss of largest infeed, f_{nadir} must remain above minimum allowed frequency levels defined by TNSPs which f_{target} in this instance.

Above calculation procedure serves as an offline process that can be used to obtain the critical inertia value of the considered power system. The framework is depicted in Fig. 2a.

B. Online SCR measurement framework

The SCR measurement sub-framework is based around the core principle mentioned in SDSCR [8]. SDSCR uses a weighted ratio given in (7) based on the impedance of renewable sources to represent the interconnections and embed into the system strength index in (8).

$$w_{m,n} = \frac{Z_{rr.m-n}}{Z_{rr,m-m}} \left(\frac{V_{r,m}}{V_{r,n}} \right) \tag{7}$$

$w_{m,n}$ is the weighted ratio between bus m and n, $Z_{rr,m-n}$ is the impedance between renewable source at bus $m-n$, $Z_{rr,m-m}$ is the impedance of the renewable connected at bus m, $V_{r,m}$ and $V_{r,n}$ are voltages in p.u. of renewable connected buses.

$$SDSCR_m = \frac{|V_{r,m}|^2}{(P_{r,m} + [\sum_{n \epsilon r, n \neq m} P_{r,n} w_{m,n}]) \times Z_{rr,mm}} \tag{8}$$

$P_{r,m}$ and $P_{r,n}$ are the active power injected by renewable sources connected at bus m and n. The impedance matrix is obtained by getting the inverse of admittance matrix (Y_{bus}) that represent the renewable connected bus network mentioned in Section III-A. The generator bus impedance matrix then can be extracted from the complete Y_{bus} matrix. The computation of $w_{m,n}$ is performed in MATLAB as an offline calculation. The SDSCR sub-framework is then implemented with real time voltage measurement of the PCC passed through a delay of $T_d = 10$ ms to account for noise and PMU delays, and lastly real time injected power from the GFMI in p.u. scale is fed to the calculation to obtain the SDSCR as an online SCR measurement at PCC. Furthermore, the critical SCR threshold will be considered as 2 thought this study [15]. The trigger framework is illustrated in Fig. 2(a). The weighted ratio ($w_{m,n}$) is calculated as 3.0856 from offline admittance matrix calculations while $Z_{rr,m-m}$ for the GFMI is 0.2 p.u.

C. Dynamic active / reactive power setpoint controller

The triggering mechanism is built around the two factors; inertia and SCR of PCC. These factors are direct indication of the PCC's system strength and system inertia behavior. Based on this, four signal conditions are created.

- $P_{Priority}$ - The standalone condition, online inertia $<$ critical inertia has to be satisfied. Q_{set} is forced to zero, prioritizing the active power contributions.
- $Q_{Priority}$ - The standalone condition, online SCR $<$ critical SCR has to be satisfied. P_{set} is forced to zero, prioritizing the reactive power contributions.
- $PQ_{Collapse}$ - The conditions, online inertia $<$ critical inertia AND online SCR $<$ critical SCR needs to be satisfied at the same time.
- $No_{Trigger}$ - Neither inertia shortfalls nor SCR shortfalls are detected. P_{set} and Q_{set} are forced to zero so that natural response of VSG control and reactive power controller is preserved to dampen the oscillations.

A 'Pick/Drop' delay mechanism is used to delay either signal pick or drop to mitigate any mode jumps caused by noise in online inertia and SCR input. In the instance of '$PQ_{collapse}$' being triggered, '$P_{priority}$' and '$Q_{priority}$' signals are isolated from the control loop proving that only one trigger type is activated at a time. The proposed dynamic controller is showed in Fig. 2(b).

III. Performance Analysis

A. Test system

The proposed framework will be tested on New England (NE) 39 bus system using DIgSILENT PowerFactory as the simulation platform. SGs at bus 32, 33, 34 and 35 are replaced by similar rated capacity wind farms with same dispatch configuration to represent a 40% renewable integrated system. The largest infeed G01, is also reduced from 10,000 MVA to 1500 MVA capacity. These modifications showcases a

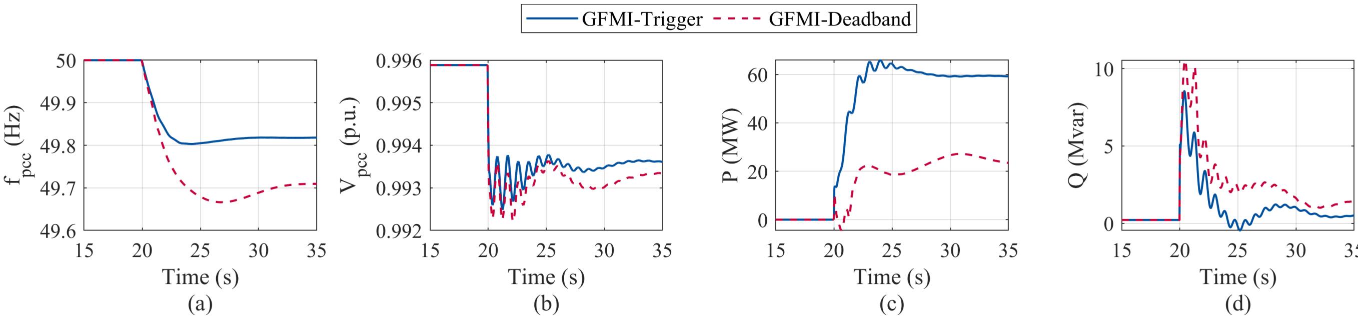

Fig. 4. Comparison of proposed GFMI framework performance for case study 1 against ‘GFMI-Deadband’. (a) frequency at PCC, (b) voltage at PCC and (c) active power dispatch.

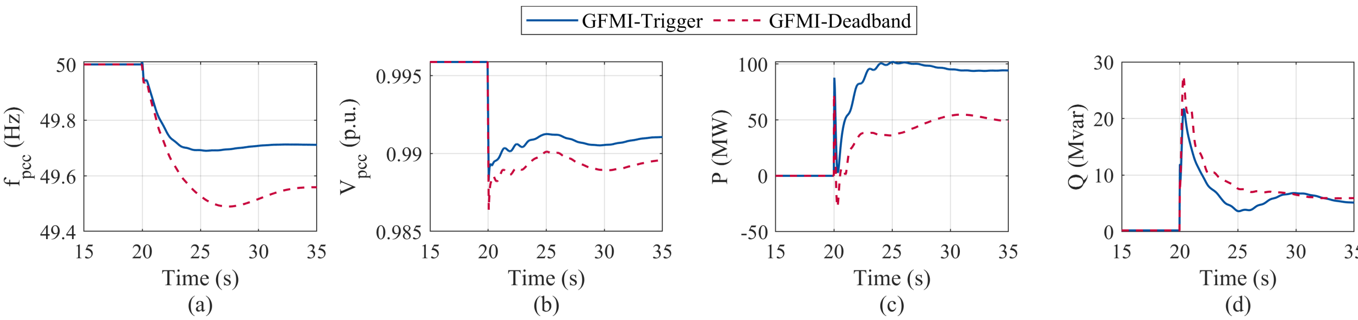

Fig. 5. Comparison of proposed GFMI framework performance for case study 2 against ‘GFMI-Deadband’. (a) frequency at PCC, (b) voltage at PCC and (c) active power dispatch.

renewable integrated weak system. The GFMI configured with the proposed framework is connected at bus 12 via a 50 km transmission line. The GFMI has a rated apparent power of 300 MVA with VSG as its grid forming control strategy. The complete framework is shown in Fig. 1 and the test system is illustrated in Fig. 3. VSG parameters are configured as follows; acceleration time constant (T_a) as 6 s and damping coefficient (D_p) as 60 p.u.

All simulations are conducted for a period of 40 s with a time step of 1 ms. The test cases are as below,

1) Case study 1 - At $t = 20$ s, SG-G10 (bus 30) is subjected to a 50% partial disconnection of capacity creating a loss of synchronous machine fault case inducing an inertia reduction of 2.1 GWs in the system. The original SG-G10 unit (1000 MVA) was remodeled as two parallel and identical 500 MVA units.
2) Case study 2 - At $t = 20$ s, an additional 200 MW load at bus 12 will be connected creating a sudden active power deficit in the system.

B. Weak grid performance

The performance of the proposed controller (shown as ‘GFMI-Trigger’) will be assessed against a GFMI equipped with VSG control configured for deadband operation (shown as ‘GFMI-Deadband’) for lower limit of NOFB. According to [16], 49.85 Hz (0.997 p.u.) is considered as the lower limit of NOFB in the NEM.

1) Case study 1: The proposed controller, labeled ‘GFMI-Trigger’, achieved a frequency nadir of 49.71 Hz at the PCC, demonstrating superior containment compared to the ‘GFMI-Deadband’ instance, which dropped to 49.67 Hz (Fig. 4(a)). This difference reflects an approximate 12.1% reduction in the maximum frequency deviation when utilizing the ‘GFMI-Trigger’ control strategy. This distinction is further confirmed in the RoCoF analysis shown in Fig. 6(a). The ‘GFMI-Deadband’ method exhibits a significant transient spike in the RoCoF immediately following the event, whereas the proposed ‘GFMI-Trigger’ instance successfully damps and arrests this rapid fluctuation, demonstrating stability. The voltage performance at the PCC (Fig. 4(b)) mirrors the improved frequency results, demonstrating superior voltage containment due to the faster control response. This performance is due to the alertness of the proposed ‘GFMI-Trigger’: it initiates its response instantaneously upon detecting the inertia and SCR collapse caused by the generator switch event at t=20 s as indicated by Fig. 7(a). In contrast, the ‘GFMI-Deadband’ utilizes a traditional frequency deadband, delaying its activation until the frequency drops below 49.85 Hz. This lag restricts the full, natural behavior of the VSG control, ultimately leading to a more pronounced voltage and frequency decline.

2) Case study 2: the ‘GFMI-Trigger’ strategy demonstrated improved frequency containment, achieving a nadir of 49.69 Hz at the PCC (Fig. 5(a)). This is a significant improvement compared to the ‘GFMI-Deadband’ strategy, which suffered a much deeper drop to 49.49 Hz. This performance represents $\sim 50\%$ reduction in the maximum frequency deviation. Furthermore, the voltage nadir and recovery is also improved as indicated by Fig. 5(b). RoCoF performance is similar in both GFMI strategies as this case study is an active power addition fault event.

979-8-3315-8138-1

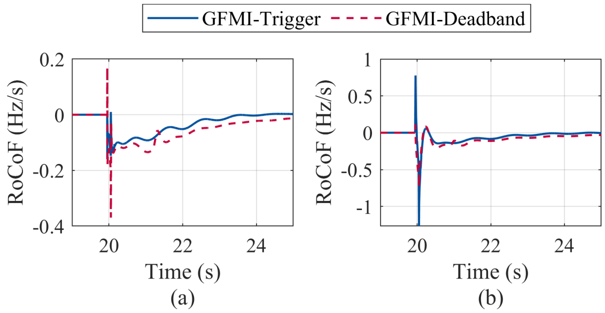

Fig. 6. RoCoF at PCC for case study 1 and 2 against proposed GFMI framework and 'GFMI-Deadband'.

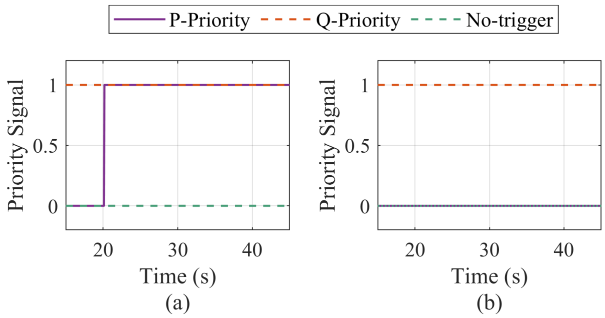

Fig. 7. Trigger signals for (a) case study 1 (b) case study 2.

C. Influence of Trigger Signal

The trigger signals for both case studies are illustrated in Fig. 7. Due to the high renewable penetration modeled in the NE 39 bus system, the '$Q_{Priority}$' signal is active from the simulation start in both scenarios, indicating a pre-fault SCR (i.e., 1.6) shortfall against the critical limit of $SCR = 2$. In Fig. 7(a), the partial generator contingency at $t = 20$ s causes not only an inertia deficit but also a voltage collapse, leading to the concurrent activation of the '$P_{Priority}$' signal. Based on the logic defined in Section II-C, this simultaneous activation triggers the '$PQ_{collapse}$' criteria, initiating full active and reactive support.

In Fig. 7(b), only the 'Q-Priority' signal is flagged for case study 2 due to weak grid conditions. The addition of 200 MW load only creates an active power deficit, hence an inertia shortfall is not detected. However, a transient is caused by measurement noise generated within the rotor speed based online inertia framework (discussed in Section II-A) because of the frequency decline at PCC. To ensure robust operation and prevent false triggering, a 'Drop-Delay' block is employed. The delay 'T_{drop}' is selected as 100 ms. This block evaluates whether the trigger signal remains TRUE for a duration of T_{drop}, effectively filtering out noise and guaranteeing that the activation is based on sustained grid weakness rather than sudden measurement spikes.

IV. Conclusion

This study successfully developed and validated a novel framework explicitly targeted at a GFMI specific market for the provision of essential system support services. We proposed and evaluated a triggering mechanism, based on real time system inertia and SCR, against traditional deadband operated systems typically used for FCAS. The results indicate that the dynamic triggering method is superior, as it effectively arrests the frequency nadir, provides faster settling times for both voltage and frequency, and significantly improves the RoCoF by eliminating control lag. This rapid responsiveness is attributed to monitoring weak grid indicators (i.e, low inertia and SCR) to be constantly on alert, rather than delaying response until frequency limits are exceeded. Furthermore, this work highlights the importance of having specialized service markets to optimally utilize their inherent dynamic characteristics, rather than being constrained by generic support mechanisms like FCAS or FFR. Future work will focus on advancing this framework by incorporating proportional support logic to enable optimal, differentiated response across multiple GFMIs.

References

[1] Y. Li, Y. Gu, and T. C. Green, "Revisiting grid-forming and grid-following inverters: A duality theory," *IEEE Trans. Power Syst.*, vol. 37, no. 6, pp. 4541–4554, 2022.

[2] C. Liyanage, I. Nutkani, and L. Meegahapola, "A comparative analysis of prominent virtual synchronous generator strategies under different network conditions," *IEEE Open Access J. Power Energy.*, vol. 11, pp. 178–195, 2024.

[3] J. Liu, Y. Miura, and T. Ise, "Comparison of dynamic characteristics between virtual synchronous generator and droop control in inverter-based distributed generators," *IEEE Trans. Power Electron.*, vol. 31, no. 5, pp. 3600–3611, 2015.

[4] M. Liu, J. Chen, and F. Milano, "On-line inertia estimation for synchronous and non-synchronous devices," *IEEE Trans. Power Syst.*, vol. 36, no. 3, pp. 2693–2701, 2021.

[5] F. Zeng, J. Zhang, Y. Zhou, and S. Qu, "Online identification of inertia distribution in normal operating power system," *IEEE Trans. Power Syst.*, vol. 35, no. 4, pp. 3301–3304, 2020.

[6] F. Zeng, J. Zhang, G. Chen, Z. Wu, S. Huang, and Y. Liang, "Online estimation of power system inertia constant under normal operating conditions," *IEEE access*, vol. 8, pp. 101 426–101 436, 2020.

[7] L. R. Goonasekara, L. Meegahapola, and S. Yan, "A comparative analysis of power system inertia estimation methods," in *2024 IEEE 34th Australasian Universities Power Engineering Conference (AUPEC)*, pp. 1–6. IEEE, 2024.

[8] D. Wu, G. Li, M. Javadi, A. M. Malyscheff, M. Hong, and J. N. Jiang, "Assessing impact of renewable energy integration on system strength using site-dependent short circuit ratio," *IEEE Trans. Sustain. Energy*, vol. 9, no. 3, pp. 1072–1080, 2018.

[9] C. Henderson, A. Egea-Alvarez, T. Kneuppel, G. Yang, and L. Xu, "Grid strength impedance metric: An alternative to scr for evaluating system strength in converter dominated systems," *IEEE Trans. Power Del.*, vol. 39, no. 1, pp. 386–396, 2024.

[10] Y. Zhu, T. C. Green, X. Zhou, Y. Li, D. Kong, and Y. Gu, "Impedance margin ratio: A new metric for small-signal system strength," *IEEE Trans. Power Syst.*, vol. 39, no. 6, pp. 7291–7303, 2024.

[11] Australian Energy Market Operator, "Guide to frequency control ancillary services," AEMO Operations, Australia, Operations Guide Version 4.0, Sep. 2025.

[12] D. Fernández-Muñoz, J. I. Pérez-Díaz, I. Guisández, M. Chazarra, and Á. Fernández-Espina, "Fast frequency control ancillary services: An international review," *Renewable and Sustainable Energy Reviews*, vol. 120, p. 109662, 2020.

[13] I. Egido, F. Fernandez-Bernal, P. Centeno, and L. Rouco, "Maximum frequency deviation calculation in small isolated power systems," *IEEE Trans. Power Syst.*, vol. 24, no. 4, pp. 1731–1738, 2009.

[14] S. Ghosh, "An estimation of coi frequency using minimal measurements in renewable power grid," *IEEE Trans. Ind. Appl.*, 2024.

[15] L. Yu, H. Sun, S. Xu, B. Zhao, and J. Zhang, "A critical system strength evaluation of a power system with high penetration of renewable energy generations," *CSEE J Power Energy*, vol. 8, no. 3, pp. 710–720, 2021.

[16] AEMO Systems Performance, "Market ancillary service specification," Australian Energy Market Operator (AEMO), Specification, Oct. 2023.

979-8-3315-8138-1